Plasmodium falciparum GCN5 plays a key role in regulating artemisinin resistance–related stress responses

Ahmad Rushdi Shakri[1#], Chengqi Wang[2#], Amuza Byaruhanga Lucky[1], Mohammad Kalamuddin[1], Anongruk Chim-Ong[1], Xiaolian Li[1], Liwang Cui[1,2], Jun Miao[1,2*]

1. Department of Internal Medicine, Morsani College of Medicine, University of South Florida, 3720 Spectrum Blvd, Tampa, FL 33612, USA

2. Center for Global Health and Infectious Diseases Research, College of Public Health, University of South Florida, 3720 Spectrum Blvd, Tampa, FL 33612, USA

Running title: PfGCN5 functions in stress response and ART resistance

# These authors contributed equally to this work.

*** Correspondence:**

Jun Miao

Phone: 813-973-7374

Email: jmiao1@usf.edu

ABSTRACT

Plasmodium falciparum causes the most severe malaria and is exposed to various environmental and physiological stresses in the human host. Given that GCN5 plays a critical role in regulating stress responses in model organisms, we aimed to elucidate PfGCN5's function in stress responses in *P. falciparum*. With TetR-DOZI conditional knockdown (KD) system, we successfully down-regulate PfGCN5 and found that KD parasites became more sensitive to heat shock, low glucose starvation, and dihydroartemisinin (DHA), the active metabolite of all artemisinin (ART) compounds. Transcriptomic analysis via RNA-seq identified 300-400 genes involved in PfGCN5-dependent, general, and stress-specific responses with high levels of overlaps among three stress conditions. Notably, using ring-stage survival assay (RSA), we found that KD or inhibition of PfGCN5 could sensitize the ART-resistant parasites to the DHA treatment. All these indicate that PfGCN5 is pivotal in regulating general and stress-specific responses in malaria parasites, implicating PfGCN5 as a potential target for malaria intervention.

IMPORTANCE Malaria leads to about half a million deaths annually and these casualties were majorly caused by the infection of *Plasmodium falciparum*. This parasite strives to survive by defending against a variety of stress conditions, such as malaria cyclical fever (heat shock), starvation due to low blood sugar (glucose) levels (hypoglycemia), and drug treatment. Previous studies have revealed that *P. falciparum* has developed unique stress responses to different stresses including ART treatment, and ART-resistant parasites harbor elevated stress responses. In this study, we provide critical evidence on the role of PfGCN5, a histone modifier, and a chromatin coactivator, in regulating general and stress-specific responses in malaria parasites, indicating that PfGCN5 can be used as a potential target for anti-malaria intervention.

INTRODUCTION

Malaria is one of the most severe public health problems worldwide. *Plasmodium falciparum* causes the most severe form of malaria and is responsible for about half a million deaths annually [1]. Malaria parasites are exposed to various environmental and physiological stresses in the human host (e.g., cyclical fever, low nutrition, and drug treatment) [2]. They have evolved general and specific mechanisms to defend against those assaults [3-5]. Several chaperones (PfHSP70-1, PfHSP70-x, PfHSP110, and the endoplasmic reticulum chaperone PfGRP170) were identified as essential proteins for the parasite to respond to heat shock (HS) [6-10]. PfAP2-HS, an ApiAP2 (AP2) domain-containing transcription factor, was found to rapidly activate *Pfhsp70-1* and *Pfhsp90* in the protective HS response [5]. Besides the conserved mechanisms for tolerance to febrile temperature and oxidative stress such as redox and protein-damage responses, parasites developed specific mechanisms such as regulating isoprenoid biosynthesis and its downstream protein modifications (geranylgeranylation and farnesylation) [4, 11]. Isoprenoid biosynthesis occurs in the apicoplast, an apicomplexan pathogen-specific organelle derived from an algal endosymbiont plastid. Many genes targeting the apicoplast were also up regulated upon HS, suggesting that the parasite utilizes an analogous defense system against heat stresses like plants [4, 12, 13].

Malaria parasites employ similar mechanisms to deal with the stresses from antimalarial treatment. ART, the first line of the anti-malaria drug, causes the production of free radical species, including reactive oxygen species (ROS), which damage proteins, lipids, and DNA [14-25]. Low-dose ART treatment was found to activate the response pathways critical for the tolerance to febrile temperature [4]. ART-resistant parasites with mutations in the Kelch protein 13 (PfK13) up-regulated genes related to stress responses (e.g., protein folding, redox, and proteasome-linked protein turnover). ART-resistant parasites respond to ART treatment by elevating gene expression related to apicoplast and mitochondrial metabolism, vesicular trafficking, lipid transport, and tRNA modifications [21-25].

GCN5 is a well-known key regulator of stress responses in the human, plants, yeast, and *Toxoplasma* by coordinating with specific transcriptional factors [26-33]. Recent studies also identified up-regulation of PfGCN5 in response to stress conditions (ART treatment, glucose starvation, and HS) along with many other up-regulated genes in *P. falciparum* [3, 34].

87 Intriguingly, PfGCN5 was found to bind many of these genes, but most of the binding sites were
88 localized in the coding regions, not in promoters. Treatment with garcinol, a PfGCN5 inhibitor,
89 sensitized the ART-resistant *P. falciparum* parasite to ART during the ring stage. In addition,
90 treating parasites with ART caused substantial changes in the abundance of active chromatin
91 markers H3K9ac and H4K8ac [35]. Collectively, these studies provided tangential evidence
92 implying PfGCN5's participation in responses to ART.

93 To elucidate the functions of PfGCN5 in orchestrating the transcriptional program in *P.*
94 *falciparum*, we deleted the C-terminal bromodomain of PfGCN5, which supposedly mediates the
95 binding of PfGCN5 to acetylated lysines. This has led to drastic transcriptional changes in many
96 genes, including protein folding-related genes and *AP2-HS* [36], suggesting that PfGCN5
97 regulates the stress response pathways. However, this assumption is undermined by the
98 dislocation of the PfGCN5 complex from its chromatin targets due to bromodomain deletion. To
99 elucidate PfGCN5's critical role in regulating stress responses in *P. falciparum*, we employed a
100 conditional knockdown (KD) system to down-regulate PfGCN5 and determined the parasite's
101 responses to different stress conditions. We provide critical evidence about the role of PfGCN5
102 in regulating general and stress-specific responses in malaria parasites, implicating PfGCN5 as a
103 potential target for therapeutic development.

104

105

106 # RESULTS

107 ## Conditional KD of PfGCN5 impairs parasite growth

108 PfGCN5 is essential for asexual blood stages, and deletion of the C-terminal bromodomain led to
109 a defect in RBC invasion and dysregulated expression of virulence genes [36]. To elucidate
110 whether and how PfGCN5 regulates stress responses, we employed the TetR-DOZI system [37,
111 38] to conditionally knock down PfGCN5 expression. We created a parasite line, TetR-
112 PfGCN5::GFP, with the insertion of the 10× aptamer in the 3' end of the endogenous PfGCN5
113 locus and fusion of the GFP tag to the PfGCN5 C-terminus, which would allow us to monitor
114 PfGCN5 expression (**Figure 1A, S1A**). Correct integration of the plasmid at the *PfGCN5* locus
115 was confirmed by a genomic Southern blot (**Figure S1B**). The binding of the TetR-DOZI to the

116 aptamer in the presence of anhydrous tetracycline (+aTc) allowed the expression of PfGCN5-
117 GFP, whereas withdrawal of aTc (-aTc) for one intraerythrocytic developmental cycle (IDC) led
118 to ~50% reduction of PfGCN5-GFP expression, shown in GFP fluorescence intensity by flow
119 cytometry analysis (**Figure 1A, 1B**). Intriguingly, the withdrawal of aTc beyond one IDC did not
120 further reduce the PfGCN5 expression level (**Figure S1C**), suggesting that parasites were
121 probably restrained from further reduction of PfGCN5 expression due to its essentiality. The -
122 aTc parasites grew significantly more slowly starting from the second cycle than the +aTc
123 parasites (**Figure 1C**). We found that PfGCN5 KD was reversible, as within ~10 h of aTc add-
124 back, the growth rate of the parasites was rapidly restored and PfGCN5-GFP expression returned
125 to the level of the +aTc culture (**Figure S1C, S1D**).

126

127 **PfGCN5 KD renders parasites more sensitive to stresses**

128 To investigate if PfGCN5 is involved in regulating stress responses, the TetR-PfGCN5::GFP
129 parasite line cultured with or without aTc was treated at the early ring stage with different stress
130 conditions: HS (41 ºC for 6 h), low glucose (0.5 g/L for 6 h), or DHA (1 μM for 12 h) (**Figure**
131 **1D-F**). After removing the stress conditions, aTc was added back to the culture, and parasite
132 growth was monitored daily. TetR-PfGCN5::GFP parasites without aTc grew significantly more
133 slowly than +aTc parasites under HS and low-glucose conditions (**Figure 1D, 1E**). After DHA
134 treatment, both +aTc and -aTc parasites were non-detectable through day 9. The +aTc culture
135 resumed growth and reached 5% parasitemia on day 15, whereas the -aTc culture had a 4-day
136 delay in reaching 5% parasitemia (**Figure 1F**). This delayed growth phenotype was not caused
137 by aTc because the 3D7 WT parasite treated the same way showed the same growth pattern after
138 DHA treatment (**Figure S1E**). Taken together, PfGCN5 KD reduced the parasite's tolerance to
139 different stresses, directly linking PfGCN5 to regulating stress responses.

140

141 **Parasites apply general and specific responses to different stresses**

142 To determine how the parasites respond to different stress conditions, we first characterize the
143 transcriptomic changes of TetR-PfGCN5::GFP parasites (+aTc) at the ring-stage (6 h post-
144 invasion, hpi) after treatment with HS (41ºC), low glucose (0.5 g/L), or DHA (30 nM) for 6 h.
145 Transcriptomic analysis was performed by RNA-seq with three biological replicates. DESeq2

146 analysis using a cutoff of > 1.5-fold and *p-adj* < 0.1 [39] identified 1183, 1130, and 1038 up-
147 regulated, as well as 1151, 1126, and 1049 down-regulated genes by HS, low-glucose, and ART
148 treatment, respectively (**Figure 2A-C, Table S1**). Surprisingly, there were substantial overlaps in
149 the up-and down-regulated genes among different stress conditions (57-65% in the up-regulated
150 genes and 70-76% in the down-regulated genes) (**Figure 2D and E, Table S1**). Gene ontology
151 (GO) enrichment analysis based on biological process (BP) (**Figure 2F**) and cellular component
152 (CC) (**Figure S2A**) showed that genes related to translation and tRNA metabolism, protein-
153 damage responses (protein folding and proteasome), glycolysis and gluconeogenesis, nucleotide
154 metabolism, host-cell remodeling, and mitochondrial and apicoplast proteins were up-regulated
155 in all stress conditions. In contrast, genes related to merozoite invasion, egression, DNA
156 replication, cytoskeleton, protein phosphorylation, and phospholipid transport were
157 downregulated, indicating that parasites used a general stress response to different stress
158 conditions (**Figure 2G, S2B**). Partial ART resistance in *P. falciparum* is medicated by mutations
159 in the propeller domain of PfK13, and the expression levels of PfK13-interacting proteins (KICs)
160 were found to influence hemoglobin uptake [40]. Intriguingly, PfK13 and seven of ten KICs
161 (KIC1-3, 5-8) were significantly down-regulated in all three stress conditions, whereas KIC4 was
162 significantly down-regulated under low glucose and KIC10 was down-regulated by both low-
163 glucose and DHA treatments (**Table S1**).

164 Transcriptomic analysis also revealed many genes whose expression was altered in a
165 stress condition-specific manner (**Figure 2F, 2G, S2A and S2B**). HS specifically induced the
166 up-regulation of genes related to the response to heat and protein unfolding, including *Pfhsp70-1*
167 and *Pfhsp90*, which are regulated by the transcription factor PfAP2-HS [5]. The low-glucose
168 condition specifically activated genes related to oxidative stress response and mitochondrial ATP
169 synthesis. ART treatment specifically up-regulated genes related to cell-cycle regulation and ER
170 stress response. Genes related to protein geranylgeranylation (apicoplast function) were only
171 enriched after HS and ART treatment but not under glucose starvation (**Figure 2F**, **Table S1**).
172 Collectively, these data indicate that different stress conditions induce specific stress responses
173 in malaria parasites.

174

175 **PfGCN5 plays a crucial role in the regulation of stress responses**

176 To understand how PfGCN5 is involved in stress responses, we sought to determine the
177 transcriptomic changes of the parasites after manipulating PfGCN5 expression in response to
178 different stress conditions. Transcriptomic analysis of the TetR-PfGCN5::GFP parasite at the
179 ring stage only identified two genes (*PfGCN5* and *EBA175*) that were significantly down-
180 regulated (> 1.5-fold, *p-adj* < 0.1) after PfGCN5 KD (-aTc), indicating that reduced PfGCN5
181 expression did not disturb the overall transcription program at the ring stage (**Table S2**). We then
182 subjected the -aTc TetR-PfGCN5::GFP parasites at 6 hpi to the same stress conditions for +aTc
183 TetR-PfGCN5::GFP parasites mentioned above for 6 h and harvested RNA for RNA-seq
184 analysis. In the -aTc parasites, the stress conditions HS, low glucose, and ART treatment resulted
185 in a similar number of genes with expression changes as in the +aTc parasites (**Figure 2**): 971,
186 1136, and 911 up-regulated genes and 922, 1170, and 1041 down-regulated genes, respectively.
187 These genes showing altered expression also overlapped substantially, with 48-60% and 66-84%
188 overlaps among the up-and down-regulated genes, respectively (**Figure 3A, 3B**, **Table S3**).

189 Comparison of the transcriptomes between the -aTc and +aTc parasites allowed us to
190 identify 2825, 2738, and 2528 genes that were differentially regulated by the HS, low glucose,
191 and DHA treatment, respectively (**Table S4**). Based on their expression patterns, these genes
192 were grouped into five clusters (**Figure 3C, Table S4**), while HS included an additional cluster
193 (VI). Cluster I and II genes were significantly down-regulated and failed to be up-regulated in -
194 aTc parasites compared to +aTc parasites under three stress conditions, respectively, suggesting
195 that these two clusters are likely the PfGCN5-dependent stress-response genes (**Figure 3C**). The
196 genes in clusters I and II are involved in many aspects of critical pathways such as translation
197 (ribosome biogenesis and tRNA modification), H3K4me3 modification, glutamine metabolism,
198 energy metabolism (ATP metabolism, glycolysis, and gluconeogenesis), drug response (ART
199 proteome, xenobiotic stimulus), protein trafficking (ER and PTEX translocon) and digestion
200 (food vacuole) (**Figure 3D**). Notably, KIC4, which was down-regulated only after glucose
201 starvation in +aTc parasites, was significantly down-regulated in -aTc parasites under all three
202 stress conditions. Similarly, GARP (glutamic acid-rich protein) expressed on the surface of
203 parasite-infected RBC [41, 42] also failed to be up-regulated in -aTc parasites under three stress
204 conditions (**Figure 3D**). Antibodies against GARP killed the parasites and were positively
205 associated with protection against severe malaria in children [43].

206 Conversely, cluster III genes, down-regulated in the +aTc parasites, were up-regulated in
207 the -aTc parasites under three stress conditions, probably to compensate for PfGCN5 KD
208 (**Figure 3D**). These include genes related to DNA replication and repair, cell cycle, and
209 isoprenoid biosynthesis. Similarly, some genes were up-regulated only by glucose starvation
210 (cell adhesion and cytoskeleton) and HS (mitochondrion electron transport). A large number of
211 genes belong to clusters IV and V, which were up- and down-regulated in the -aTc parasites
212 under stress conditions in the same trends as in the +aTC parasite, respectively, suggesting that
213 these genes may be PfGCN5-independent. HS induced a new cluster of genes (VI), which were
214 up-regulated in the -aTc parasites but no change in the +aTc parasites (**Figure 3C**). These genes
215 are involved in similar pathways as the cluster III genes, suggesting that HS might have involved
216 more genes in compensation for PfGCN5 KD (**Table S4**). By comparing the overlaps within
217 these clusters upon three different stress conditions, low levels of overlaps were found among
218 PfGCN5-dependent stress-response genes (cluster I and II) and the KD compensation-related
219 genes (cluster III), whereas high levels of overlaps among the PfGCN5-independent stress-
220 response genes (cluster IV and V) were identified (**Figure S3, Table S4**), suggesting PfGCN5-
221 dependent stress responses are also stress-condition-specific to a certain degree. Genes related to
222 the HSP70 cycle, P-bodies, and translation initiation were down-regulated (cluster I) in -aTc
223 parasites specifically under glucose starvation, while genes related to protein
224 geranylgeranylation, isoprenoid biosynthesis, proteasome assembly, and mitochondrion transport
225 and targeting failed to be up-regulated in -aTc parasites under DHA treatment. Likewise, genes
226 related to cation homeostasis (pH reduction) and hemoglobin digestion failed to be up-regulated
227 in -aTc parasites under low glucose and HS, respectively (**Figure 3D**). Collectively, these data
228 demonstrate that PfGCN5 regulates stress response by targeting general and stress condition-
229 specific stress response genes.

230

231 **PfGCN5 KD reduces parasites' tolerance to DHA treatment**

232 Growth recovery assay and transcriptomic analysis after DHA treatment indicated PfGCN5's
233 involvement in regulating general and specific responses to DHA (**Figure 1F, 3D**). To translate
234 this phenotype into ART sensitivity, we performed the ring-stage survival assay (RSA) with
235 TetR-PfGCN5::GFP parasites. The TetR-PfGCN5::GFP (-aTc) parasites at the early ring were

236 exposed to 700 nM DHA for 6 h, and aTc was added back right after DHA treatment to exclude
237 the subsequent effect of PfGCN5 KD on parasite growth defect. Compared to the RSA value of
238 the TetR-PfGCN5::GFP parasites under the +aTc conditions, PfGCN5 KD resulted in a ~60%
239 reduction in the RSA value (**Figure 4A**).

240 With the demonstration of PfGCN5's role in regulating parasite's responses to ART
241 drugs, we wanted to test if inhibition of PfGCN5's enzymatic activity would re-sensitize ART-
242 resistant parasites to ART drugs. We evaluated butyrolactone 3 (MB-3), which we showed
243 previously to inhibit PfGCN5's enzymatic activity with an IC_{50} of ~125 μM [44]. With the
244 standard SYBR green I growth inhibition assay, MB-3 inhibited 3D7 parasites at an IC_{50} of ~
245 27.5 μM. We found that a 6-h exposure of Cam2, an ART-resistant strain collected from
246 Cambodia with the K13 C580Y mutation (MRA-1236), at the early-ring stage to 10.9, 17.3, and
247 27.5 μM of MB-3, corresponding to the IC_{10}, IC_{25}, and IC_{50} concentrations of the drug,
248 respectively, did not cause noticeable changes in the survival rate of ART-resistant strain as
249 compared to the DMSO vehicle control (**Figure 4B**). Whereas RSA of Cam2 showed a survival
250 rate of 13%, co-incubation of DHA and MB-3 for 6 h significantly reduced the RSA value in an
251 MB-3 concentration-dependent manner compared to DHA treatment only (**Figure 4D**). Taken
252 together, these data showed that KD or inhibition of PfGCN5 could re-sensitize the ART-
253 resistant parasites to ART drugs.

254

255 **DISCUSSION**

256 This study aimed to confirm PfGCN5's involvement in regulating stress responses in the malaria
257 parasite and gain a mechanistic understanding of PfGCN5's role in responding to different stress
258 conditions. Using a conditional KD system, we successfully down-regulated PfGCN5 expression
259 and showed that PfGCN5 KD increased the parasite's susceptibility to all stress conditions used,
260 emphasizing PfGCN5's central role in stress response. Through transcriptomic analysis, we
261 identified 300-400 genes involved in PfGCN5-dependent, general, and stress-specific responses.
262 Furthermore, using growth recovery assay and RSA, we found that KD or inhibition of PfGCN5
263 could sensitize the ART-resistant parasites to the ART treatment.

264 In addition to the parasite-specific functions of PfGCN5 in regulating invasion and
265 virulence in *P. falciparum*, we confirm an evolutionarily conserved role of PfGCN5 in regulating

266 stress responses. We have shown that the malaria parasites can mount a rapid stress response,
267 with the expression of >2,000 genes altered under each stress condition tested. Importantly, there
268 were significant overlaps in the differentially expressed genes among the different stresses,
269 highlighting the presence of a shared general mechanism. By comparing gene expression
270 between PfGCN5-normal and PfGCN5-deficient parasites exposed to stresses, we identified a
271 subset of 300-400 genes whose expression in response to stresses depended on PfGCN5. These
272 genes are involved in common stress responses (e.g., translation and ribosome, tRNA, and ATP
273 metabolic process, glycolysis, gluconeogenesis, protein geranylgeranylation, proteasome
274 assembly, Sec61 translocon, isoprenoid biosynthesis, food vacuole, apoptosis, and
275 mitochondrion targeting) and stress-specific response (e.g., P-bodies, protein folding, and
276 mitochondrion targeting upon starvation, HS, and ART treatment, respectively). Especially,
277 seven K13-interacting proteins (KICs) involved in ART resistance by participating in
278 hemoglobin uptake [40] were down-regulated under all three stress conditions. Furthermore,
279 KIC4 was dysregulated in PfGCN5 KD parasites during stress, indicating that the K13 regulatory
280 pathway is a common stress response. Similarly, a large-scale forward-genetic screen in *P.*
281 *falciparum* revealed apicoplast-targeted proteins including isoprenoid biosynthesis and its
282 downstream protein modifications (geranylgeranylation and farnesylation) as a common pathway
283 mediating tolerance to febrile temperature, a low dose of ART, and oxidative stress [4, 11].
284 Likewise, ART-resistant parasites showed elevated stress responses [4, 21-25]. In addition, this
285 study also identified stress-specific responses, such as upregulation of *Pfhsp70-1* and *Pfhsp90*
286 after HS, ATP synthesis under starvation, and ER stress response after ART treatment. These
287 data highlight that the malaria parasite has evolved an integrated mechanism responding to
288 different stress conditions, and PfGCN5 is a key activator of general and specific stress
289 responses.

290 PfGCN5 is present in a large coactivator protein complex(es) to regulate global gene
291 expression in *P. falciparum* [36]. Activation of specific pathways by PfGCN5 may be conferred
292 by specific transcription factors such as the AP2-domain proteins. In the PfGCN5 complex,
293 PfAP2-LT is present as a consistent member, and other AP2 TFs (e.g., AP2-I and
294 PF3D7_1239200) have also been found in PfGCN5 pulldowns [36, 45]. Of particular relevance,
295 PfAP2-HS was found to play a key role in the HS response through the activation of *Pfhsp70-1*
296 and *Pfhsp90* [5]. While we hypothesize that the PfGCN5 complex may be dynamically recruited

297 to activate genes in the stress response pathways by PfAP2-HS, the exact mechanism remains to
298 be tested.

299 The finding of PfGCN5 KD resulting in delayed recovery and lower RSA rate upon DHA
300 exposure is consistent with the reflection of the partial ART resistance phenotype in the general
301 elevation of stress tolerance as typically occurring in an early phase of resistance [46]. Re-
302 sensitization of the ART-resistant parasites by chemically inhibiting PfGCN5 may provide a way
303 to deal with the emerging problem of ART resistance in endemic areas and underline PfGCN5 as
304 a potential target for therapeutic development.

305

306 # MATERIAL AND METHODS

307 **Parasite culture**

308 The *P. falciparum* strain 3D7 and its genetically modified clones were cultured at 37°C in a gas
309 mixture of 5% CO_2, 3% O_2 and 92% N_2 with type O^+ RBCs at 5% hematocrit in RPMI 1640
310 medium supplemented with 25 mM $NaHCO_3$, 25 mM HEPES, 50 mg/L hypoxanthine, 2 g/L
311 glucose, 0.5% Albumax II and 40 mg/ml gentamicin sulfate [47]. Synchronization of asexual
312 stages was performed by sorbitol treatment at the rings stage followed by incubation of
313 synchronized schizonts with fresh RBCs for 3 h to obtain highly synchronized ring-stage
314 parasites [48].

315 **Genetic manipulation of *PfGCN5***

316 To generate a PfGCN5 KD parasite line by TetR-DOZI system, a *PfGCN5* fragment [nucleotides
317 (nt) 3778-4758] was amplified using primers F1 (GAGCGCGCTGTTACCTCAACTGAGC,
318 *BssH*II underlined) and R1 (GAGGTTACCTGCTGTATCAGTTATAGCTTC, *BstE*II
319 underlined) from *P. falciparum* genomic DNA and cloned into pMG75 ATPase4 plasmid [37,
320 38] to replace the ATPase4 fragment and generate pMG75-PfGCN5. To fuse the C-terminal of
321 PfGCN5 with GFP, we amplified GFP using primers F2
322 (CAGGTTACCATGAGTAAAGGAGAAGAACTTTTC, *BstE*II underlined) and R2
323 (CTGACGTCTTATTTGTATAGTTCATCCATGCC, *Aat*II underlined) and cloned it into
324 pMG75-PfGCN5 at the *BstE*II and *Aat*II sites.

325 Parasite transfection was done using the RBC loading method [49]. Briefly, 100 μg of

326 plasmid was introduced into fresh RBCs by electroporation. Purified schizonts were used to
327 infect the RBCs pre-loaded with the plasmid, and selection was done with blasticidin (BSD) at
328 2.5 μg/mL for approximately 4 weeks with weekly replenishment of fresh RBCs until resistant
329 parasites appeared. Resistant parasites were subjected to three cycles of drug on-off selection and
330 single clones of parasites with stable integration of the constructs were obtained by limiting
331 dilution [48]. aTc at 0.5 μM was constantly added to the culture to maintain adequate expression
332 of *PfGCN5*. GFP-positive parasites were sorted and cloned by fluorescence-activated cell
333 sorting. Correct integrations of plasmids into the parasite genome were screened by Southern
334 blot with the digoxigenin (DIG)-labeled probes using an established protocol [36, 50]. The probe
335 was generated by using the F1 and R1 primers.

336 **PfGCN5 KD and growth phenotype analysis**

337 Flow cytometry was used to measure the GFP level in the TetR-PfGCN5::GFP parasites. The
338 growth of the TetR-PfGCN5::GFP parasite line was measured in triplicate. Cultures were tightly
339 synchronized, as described above. The parasitemia of culture was monitored daily by microscopy
340 of Giemsa-stained blood smears. Growth rates after *PfGCN5* KD were analyzed by starting
341 cultures at 0.1% rings with the vehicle control (ethanol, -aTc) or aTc (+aTc) for seven days.
342 Growth rates after HS and low glucose treatment (6 h) were measured by starting cultures at
343 0.5% rings with the vehicle control (-aTc) or aTc for five days. Parasite recovery assay was
344 performed as described previously by treating 2% early ring-stage parasites with 1 μM of DHA
345 for 12 h [51]. aTc was added back to the PfGCN5 KD (-aTc) culture after removing stress
346 conditions.

347 **Transcriptome analysis**

348 To compare the parasites' transcriptomes upon stress conditions, we performed RNA-seq
349 analysis using the ring-stage TetR-GCN5::GFP parasites with or without aTc. The experiment
350 was done in 2-3 replicates. Total RNA was extracted using the ZYMO RNA purification kit and
351 RNA integrity was confirmed by the TapeStation system (Agilent). Total RNA was used to
352 generate the sequencing libraries using the KAPA Stranded mRNA Seq kit for the Illumina
353 sequencing platform according to the manufacturer's protocol (KAPA biosystems). Libraries
354 were sequenced on an Illumina NextSeq 550 using 150 nt paired-end sequencing. Reads from
355 Illumina sequencing were mapped to the *P. falciparum* genome sequence (Genedb v3.1) using

356 HISAT2 [52]. The expression levels and the differential expression were calculated by
357 FeatureCounts and DESeq2 [53, 54] with the criteria of ≥ 1.5-fold of alteration and *p*-adjustment
358 <0.1. RNA-seq data were submitted to the NCBI GEO repository (accession number
359 GSE221211) with a token (cxmngauyrvcfjqj) for reviewers' accession.

360 **GO enrichment analysis and clustering**

361 The GO enrichment was performed on PlasmDB (https://plasmodb.org/plasmo/). The fold
362 changes of gene expressions were further normalized by Z-score, and K-means were performed
363 to identify differential gene expression patterns among the transcriptomes with or without KD of
364 PfGCN5 under different stress conditions.

365 ***In vitro* drug assay and RSA**

366 The standard SYBR Green I-based fluorescence assay [55, 56] was used to assess parasite
367 susceptibilities to MB-3. Synchronized cultures at the ring stage were diluted with fresh
368 complete medium to 1% hematocrit and 0.5% parasitemia. *In vitro* drug assays were performed
369 in 96-well microtiter plates with serially diluted drug concentrations. Three technical and
370 biological replications were performed.

371 RSA was performed as previously described [56-60]. Briefly, schizonts were purified
372 from tightly synchronized cultures using a Percoll gradient and allowed to rupture and invade
373 fresh RBCs for 3 h. The cultures were treated with sorbitol to select early rings and eliminate the
374 remaining schizonts. Ring-stage parasites of 0-3 hpi at 1% parasitemia and 1% hematocrit were
375 exposed to 700 nM DHA for 6 h, followed by a single wash. MB-3 was added and washed
376 simultaneously as DHA, and aTc was added back to the PfGCN5 KD (-aTc) culture after drug
377 treatment. After culturing for 66 h, ~10,000 RBCs were observed on thin blood smears to count
378 viable parasites.

379 **Statistical analysis**

380 For all experiments, three or more independent biological replicates were performed. The results
381 were presented as mean ± SD. Results were regarded as significant if $P < 0.05$ as established by
382 T-test, and the respective analysis was shown in the figure legends.

383

Acknowledgments

This study was supported by the startup fund from Morsani College of Medicine, University of South Florida, and grant R21AI149202 from the National Institute of Allergy and Infectious Diseases (NIAID), NIH, USA to JM, and grants R01AI128940 and U19AI089672 from NIAID, NIH, USA to LC. We are grateful to Jacobus *Pharmaceuticals* for providing the drug WR99210. We thank the University of South Florida Genomics Program (Sequencing Core and Computational Core/Omics Hub) for supporting NGS sequence and data analysis.

Author Contributions

J.M. conceived and designed the study. AR.S, C.W., and AB.L. performed research, acquired and analyzed data. C.W. analyzed the RNA-seq data. M.K. and A.C. assisted research. X.L. conducted parasite culture and phenotypic growth analysis. J.M. wrote the original draft. L.C. revised the manuscript.

Declaration of Interests

The authors declare no competing interests.

REFERENCES

1. WHO, *Would Malaria Report 2021.* Geneva: WHO, 2021.
2. Brown, A.C. and J.L. Guler, *From Circulation to Cultivation: Plasmodium In Vivo versus In Vitro.* Trends in Parasitology, 2020. **36**(11): p. 914-926.
3. Rawat, M., et al., *Histone acetyltransferase PfGCN5 regulates stress responsive and artemisinin resistance related genes in Plasmodium falciparum.* Sci Rep, 2021. **11**(1): p. 852.
4. Zhang, M., et al., *The apicoplast link to fever-survival and artemisinin-resistance in the malaria parasite.* Nat Commun, 2021. **12**(1): p. 4563.
5. Tinto-Font, E., et al., *A heat-shock response regulated by the PfAP2-HS transcription factor protects human malaria parasites from febrile temperatures.* Nat Microbiol, 2021. **6**(9): p. 1163-1174.
6. Dutta, T., et al., *Exported plasmodial J domain protein, PFE0055c, and PfHsp70-x form a specific co-chaperone-chaperone partnership.* Cell Stress & Chaperones, 2021. **26**(2): p. 355-366.
7. Day, J., et al., *The Plasmodium falciparum Hsp70-x chaperone assists the heat stress response of the malaria parasite.* Faseb Journal, 2019. **33**(12): p. 14611-14624.
8. Kudybah, H.M., et al., *The endoplasmic reticulum chaperone PfGRP170 is essential for asexual development and is linked to stress response in malaria parasites.* Cellular Microbiology, 2019. **21**(9).
9. Lu, K.Y., et al., *Phosphatidylinositol 3-phosphate and Hsp70 protect Plasmodium falciparum from heat-induced cell death.* Elife, 2020. **9**.

419 10. Muralidharan, V., et al., *Plasmodium falciparum heat shock protein 110 stabilizes the asparagine*
420 *repeat-rich parasite proteome during malarial fevers.* Nature Communications, 2012. **3**.
421 11. Mathews, E.S., A.J. Jezewski, and A.R.O. John, *Protein Prenylation and Hsp40 in Thermotolerance*
422 *of Plasmodium falciparum Malaria Parasites.* Mbio, 2021. **12**(3).
423 12. Boucher, M.J., et al., *Integrative proteomics and bioinformatic prediction enable a high-*
424 *confidence apicoplast proteome in malaria parasites.* Plos Biology, 2018. **16**(9).
425 13. Foth, B.J., et al., *Dissecting apicoplast targeting in the malaria parasite Plasmodium falciparum.*
426 Science, 2003. **299**(5607): p. 705-708.
427 14. Haynes, R.K., et al., *Considerations on the mechanism of action of artemisinin antimalarials: part*
428 *1--the 'carbon radical' and 'heme' hypotheses.* Infect Disord Drug Targets, 2013. **13**(4): p. 217-77.
429 15. Heller, L.E. and P.D. Roepe, *Artemisinin-Based Antimalarial Drug Therapy: Molecular*
430 *Pharmacology and Evolving Resistance.* Trop Med Infect Dis, 2019. **4**(2).
431 16. Klonis, N., D.J. Creek, and L. Tilley, *Iron and heme metabolism in Plasmodium falciparum and the*
432 *mechanism of action of artemisinins.* Curr Opin Microbiol, 2013. **16**(6): p. 722-7.
433 17. Heller, L.E., E. Goggins, and P.D. Roepe, *Dihydroartemisinin-Ferriprotoporphyrin IX Adduct*
434 *Abundance in Plasmodium falciparum Malarial Parasites and the Relationship to Emerging*
435 *Artemisinin Resistance.* Biochemistry, 2018. **57**(51): p. 6935-6945.
436 18. Gopalakrishnan, A.M. and N. Kumar, *Antimalarial action of artesunate involves DNA damage*
437 *mediated by reactive oxygen species.* Antimicrob Agents Chemother, 2015. **59**(1): p. 317-25.
438 19. Krungkrai, S.R. and Y. Yuthavong, *The antimalarial action on Plasmodium falciparum of*
439 *qinghaosu and artesunate in combination with agents which modulate oxidant stress.* Trans R
440 Soc Trop Med Hyg, 1987. **81**(5): p. 710-4.
441 20. Wang, J., et al., *Artemisinin directly targets malarial mitochondria through its specific*
442 *mitochondrial activation.* PLoS One, 2010. **5**(3): p. e9582.
443 21. Mok, S., et al., *Artemisinin-resistant K13 mutations rewire Plasmodium falciparum's intra-*
444 *erythrocytic metabolic program to enhance survival.* Nat Commun, 2021. **12**(1): p. 530.
445 22. Mok, S., et al., *Population transcriptomics of human malaria parasites reveals the mechanism of*
446 *artemisinin resistance.* Science, 2015. **347**(6220): p. 431-435.
447 23. Bridgford, J.L., et al., *Artemisinin kills malaria parasites by damaging proteins and inhibiting the*
448 *proteasome.* Nature Communications, 2018. **9**.
449 24. Rocamora, F., et al., *Oxidative stress and protein damage responses mediate artemisinin*
450 *resistance in malaria parasites.* Plos Pathogens, 2018. **14**(3).
451 25. Cui, L., et al., *Mechanisms of in vitro resistance to dihydroartemisinin in Plasmodium falciparum.*
452 Mol Microbiol, 2012. **86**(1): p. 111-28.
453 26. Gaupel, A.C., T.J. Begley, and M. Tenniswood, *Gcn5 Modulates the Cellular Response to*
454 *Oxidative Stress and Histone Deacetylase Inhibition.* J Cell Biochem, 2015. **116**(9): p. 1982-92.
455 27. Hu, Z., et al., *Histone acetyltransferase GCN5 is essential for heat stress-responsive gene*
456 *activation and thermotolerance in Arabidopsis.* Plant J, 2015. **84**(6): p. 1178-91.
457 28. Johnsson, A., et al., *Stress-specific role of fission yeast Gcn5 histone acetyltransferase in*
458 *programming a subset of stress response genes.* Eukaryot Cell, 2006. **5**(8): p. 1337-46.
459 29. Naguleswaran, A., et al., *Toxoplasma gondii lysine acetyltransferase GCN5-A functions in the*
460 *cellular response to alkaline stress and expression of cyst genes.* PLoS Pathog, 2010. **6**(12): p.
461 e1001232.
462 30. Mutlu, B. and P. Puigserver, *GCN5 acetyltransferase in cellular energetic and metabolic*
463 *processes.* Biochimica Et Biophysica Acta-Gene Regulatory Mechanisms, 2021. **1864**(2).
464 31. Gan, L., et al., *Updated Mechanisms of GCN5-The Monkey King of the Plant Kingdom in Plant*
465 *Development and Resistance to Abiotic Stresses.* Cells, 2021. **10**(5).

466 32. Xue-Franzen, Y., et al., *Genome-wide characterisation of the Gcn5 histone acetyltransferase in*
467 *budding yeast during stress adaptation reveals evolutionarily conserved and diverged roles.* Bmc
468 Genomics, 2010. **11**.
469 33. Hsieh, W.C., et al., *Glucose starvation induces a switch in the histone acetylome for activation of*
470 *gluconeogenic and fat metabolism genes.* Mol Cell, 2022. **82**(1): p. 60-74 e5.
471 34. Rawat, M., et al., *Role of PfGCN5 in nutrient sensing and transcriptional regulation in*
472 *Plasmodium falciparum.* J Biosci, 2020. **45**.
473 35. Gupta, D.K., et al., *DNA damage regulation and its role in drug-related phenotypes in the malaria*
474 *parasites.* Sci Rep, 2016. **6**: p. 23603.
475 36. Miao, J., et al., *A unique GCN5 histone acetyltransferase complex controls erythrocyte invasion*
476 *and virulence in the malaria parasite Plasmodium falciparum.* PLoS Pathog, 2021. **17**(8): p.
477 e1009351.
478 37. Goldfless, S.J., J.C. Wagner, and J.C. Niles, *Versatile control of Plasmodium falciparum gene*
479 *expression with an inducible protein-RNA interaction.* Nat Commun, 2014. **5**: p. 5329.
480 38. Ganesan, S.M., et al., *Synthetic RNA-protein modules integrated with native translation*
481 *mechanisms to control gene expression in malaria parasites.* Nat Commun, 2016. **7**: p. 10727.
482 39. Love, M.I., W. Huber, and S. Anders, *Moderated estimation of fold change and dispersion for*
483 *RNA-seq data with DESeq2.* Genome Biol, 2014. **15**(12): p. 550.
484 40. Birnbaum, J., et al., *A Kelch13-defined endocytosis pathway mediates artemisinin resistance in*
485 *malaria parasites.* Science, 2020. **367**(6473): p. 51-59.
486 41. Davies, H.M., K. Thalassinos, and A.R. Osborne, *Expansion of Lysine-rich Repeats in Plasmodium*
487 *Proteins Generates Novel Localization Sequences That Target the Periphery of the Host*
488 *Erythrocyte.* Journal of Biological Chemistry, 2016. **291**(50): p. 26188-26207.
489 42. Almukadi, H., et al., *Human erythrocyte band 3 is a host receptor for Plasmodium falciparum*
490 *glutamic acid-rich protein.* Blood, 2019. **133**(5): p. 470-480.
491 43. Raj, D.K., et al., *Anti-PfGARP activates programmed cell death of parasites and reduces severe*
492 *malaria.* Nature, 2020. **582**(7810): p. 104-+.
493 44. Chen, Z., et al., *Arbitrarily Accessible 3D Microfluidic Device for Combinatorial High-Throughput*
494 *Drug Screening.* Sensors (Basel), 2016. **16**(10).
495 45. Santos, J.M., et al., *Red Blood Cell Invasion by the Malaria Parasite Is Coordinated by the PfAP2-I*
496 *Transcription Factor.* Cell Host Microbe, 2017. **21**(6): p. 731-741 e10.
497 46. Wellems, T.E., et al., *'Artemisinin Resistance': Something New or Old? Something of a Misnomer?*
498 Trends in Parasitology, 2020. **36**(9): p. 735-744.
499 47. Trager, W. and J.B. Jensen, *Human malaria parasites in continuous culture.* Science, 1976.
500 **193**(4254): p. 673-5.
501 48. Miao, J. and L. Cui, *Rapid isolation of single malaria parasite-infected red blood cells by cell*
502 *sorting.* Nat Protoc, 2011. **6**(2): p. 140-6.
503 49. Deitsch, K., C. Driskill, and T. Wellems, *Transformation of malaria parasites by the spontaneous*
504 *uptake and expression of DNA from human erythrocytes.* Nucleic Acids Res, 2001. **29**(3): p. 850-
505 3.
506 50. Miao, J., et al., *The Puf-family RNA-binding protein PfPuf2 regulates sexual development and sex*
507 *differentiation in the malaria parasite Plasmodium falciparum.* J Cell Sci, 2010. **123**(Pt 7): p.
508 1039-49.
509 51. Liang, X., et al., *A Leak-Free Inducible CRISPRi/a System for Gene Functional Studies in*
510 *Plasmodium falciparum.* Microbiol Spectr, 2022: p. e0278221.
511 52. Kim, D., B. Langmead, and S.L. Salzberg, *HISAT: a fast spliced aligner with low memory*
512 *requirements.* Nat Methods, 2015. **12**(4): p. 357-60.

513 53. Anders, S. and W. Huber, *Differential expression analysis for sequence count data.* Genome Biol,
514 2010. **11**(10): p. R106.
515 54. Liao, Y., G.K. Smyth, and W. Shi, *featureCounts: an efficient general purpose program for*
516 *assigning sequence reads to genomic features.* Bioinformatics, 2014. **30**(7): p. 923-30.
517 55. Smilkstein, M., et al., *Simple and inexpensive fluorescence-based technique for high-throughput*
518 *antimalarial drug screening.* Antimicrobial Agents and Chemotherapy, 2004. **48**(5): p. 1803-
519 1806.
520 56. Wang, Z.L., et al., *Artemisinin Resistance at the China-Myanmar Border and Association with*
521 *Mutations in the K13 Propeller Gene.* Antimicrobial Agents and Chemotherapy, 2015. **59**(11): p.
522 6952-6959.
523 57. Witkowski, B., et al., *Novel phenotypic assays for the detection of artemisinin-resistant*
524 *Plasmodium falciparum malaria in Cambodia: in-vitro and ex-vivo drug-response studies.* Lancet
525 Infectious Diseases, 2013. **13**(12): p. 1043-1049.
526 58. Siddiqui, F.A., et al., *Plasmodium falciparum Falcipain-2a Polymorphisms in Southeast Asia and*
527 *Their Association With Artemisinin Resistance.* Journal of Infectious Diseases, 2018. **218**(3): p.
528 434-442.
529 59. Straimer, J., et al., *Plasmodium falciparum K13 Mutations Differentially Impact Ozonide*
530 *Susceptibility and Parasite Fitness In Vitro.* Mbio, 2017. **8**(2).
531 60. Siddiqui, F.A., et al., *Role of Plasmodium falciparum Kelch 13 Protein Mutations in P. falciparum*
532 *Populations from Northeastern Myanmar in Mediating Artemisinin Resistance.* mBio, 2020.
533 **11**(1).

534 # FIGURE LEGENDS

535

536 **Figure 1. KD of PfGCN5 led to parasite growth defects and increased susceptibilities to**
537 **stress conditions**. **A**. A diagram illustrates the TetR-DOZI inducible KD system, where 10x
538 aptamer motifs are inserted into the 3' UTR of the *PfGCN5*. Adding aTc causes TetR-DOZI to be
539 released from the aptamer, inducing protein translation (translation "ON"), whereas withdrawal
540 of aTc leads to the binding of TetR-DOZI to the aptamer motifs to block the translational process
541 (translation "OFF"), “AAAAA” indicates the polyA tail of the mRNA. **B**. Measurement of GFP
542 expression in the TetR-PfGCN5:GFP parasites by flow cytometry. The reduction of PfGCN5-
543 GFP protein level after withdrawal of aTc for 48 h is shown. **C**. The growth curves of TetR-
544 PfGCN5:GFP parasites with or without aTc. The parasite growth rates were significantly
545 reduced after KD of PfGCN5 (-aTc) compared to the parasites without KD of PfGCN5 (+aTc) (p
546 < 0.001, multiple T-test). **D** and **E**. Parasite growth with or without *PfGCN5* KD exposed to heat
547 shock (**D**) and low glucose (**E**) conditions, respectively. (**: $p < 0.01$, *** : $p < 0.001$, multiple
548 T-test). TetR-PfGCN5:GFP parasites at the early ring stage with (+aTc) or without aTc (-aTc)
549 were treated by HS (41 ºC) and low-glucose (0.5 g/L) for 6 h. aTc was added back to the culture
550 after stress treatment. **F**. Parasite recovery assays showing the time required for the control
551 (+aTC) or the PfGCN5 KD (-aTc) parasites to recover after treatment with 1 μM of DHA for 12
552 h ($p < 0.001$, multiple T-test). aTc was added back to the culture immediately after DHA
553 treatment.

554

555 **Figure 2. Transcriptional changes of +aTc TetR-PfGCN5::GFP parasites upon exposure to**
556 **different stress conditions**. **A**-**C**. Volcano plots showing differentially expressed genes at the
557 ring stage after treatment with heat shock (HS) (**A**), low glucose (L-Glu) (**B**), and DHA (**C**). **D**
558 and **E**. Venn diagrams showing the extent of overlaps among the up- (**D**) and down- (**E**)
559 regulated genes upon HS, low glucose, and DHA treatments, respectively. **F** and **G**. Heatmaps
560 display the GO enrichment analyses of up- (**F**) and down-(**G**) regulated genes upon HS, low
561 glucose, and DHA treatments based on the biological process (BP), showing the common and
562 stress-specific stress responses.
563
564 **Figure 3. Transcriptomic analyses of PfGCN5-dependent stress responses**. **A** and **B**. Venn
565 diagrams showing the overlaps among the up- (**A**) and down- (**B**) regulated genes upon DHA, HS,
566 and low-glucose treatments in the -aTc (PfGCN5 KD) parasites, respectively. **C**. Heatmaps show
567 the expression patterns (Exp) in WT (+aTc) and PfGCN5 KD (-aTc) parasites upon HS, low
568 glucose (L-Glu), and DHA treatments. ↑, ↓, and − denote genes that were up-, down-, and not-
569 altered after treatments, ↗ indicates the genes failed to be up-regulated in PfGCN5 KD parasite
570 after ART treatment. #: numbers of genes in each cluster. **D**. GO enrichment analyses of genes in
571 different clusters. The GO terms shared among the three stress conditions are shown in bold and
572 black color, while stress-specific enrichments are listed by words in red, blue, and green for HS,
573 low glucose, and DHA treatments, respectively.

574 **Figure 4. KD or inhibitor of PfGCN5 sensitized the parasites to DHA treatments**. **A**. RSA of
575 +aTc and -aTc parasites (TetR-PfGCN5::GFP) indicates that KD of PfGCN5 by the withdrawal of
576 aTc (-aTc) led to the reduction of RSA values ($p < 0.01$, T-test). RSAs of +aTc parasite (~0.3%)
577 were set up as 100% for comparison. aTc was added back to the culture after 6 h treatment by
578 700nM DHA. **B** and **C**. RSA of an ART-resistant K13 mutant strain (isolated from Cambodia with
579 C580Y mutation) while MB-3 was added and withdrawn at the same time as DHA treatment. MB-
580 3 at the concentrations of IC_{10} (10.9 μM), IC_{25} (17.3 μM), and IC_{50} (27.5 μM) without DHA did
581 not cause any noticeable alteration of RSA value as compared to DMSO vehicle control (**C**)
582 whereas co-incubation with both DHA and MB-3 significantly reduced RSA rate compared to
583 DHA treatment only (**D**) (**: $p < 0.01$, *** : $p < 0.001$, T-test).

584

585 **Figure S1. PfGCN5 knockdown using the TetR-DOZI system**. **A.** Schematic diagram shows
586 the insert of 10 x aptamer (A*) in 3' UTR of *PfGCN5* and integration of the TetR-DOZI expression
587 cassette by single-crossover homologous recombination. KAT, lysine acetyltransferase domain;
588 ADA2, ADA2-binding domain; BrD, bromodomain; H, HindIII restriction site. The recombined
589 PfGCN5 locus includes GFP tagging at the C-terminus of PfGCN5. **B.** Southern blot indicates
590 three positive clones from transfected parasites. M, molecular markers in Kb. **C.** Recovery of
591 PfGCN5-GFP expression after adding aTc back to the KD parasite culture for 2-10h. The KD
592 parasites were cultured without aTc (-aTc) for 5 IDCs before adding aTc. The PfGCN5-GFP

593 expression was measured by detecting the GFP level in the parasites via flow cytometry. The
594 median GFP levels of 5000 parasites were used for each replicate. The percentage of GFP level
595 compared to parasite cultured without withdrawal of aTc (+aTc). **D**. The growth rates of parasites
596 without KD of PfGCN5 (+aTc) and parasites with re-storage of PfGCN5 expression by adding aTc
597 back to the -aTc parasites (+aTc post KD). **E**. Growth recovery assays after 1μM of DHA treatment
598 of 3D7 with and without –aTc.

599 **Figure S2. Drastic transcriptional changes upon stress conditions**. **A** and **B**. Heatmaps
600 display the GO enrichment analyses of up- (**A**) and down- (**B**) regulated genes upon HS and low
601 glucose (L-Glu), and DHA treatments based on the cellular component (CC) showing the
602 common and stress-specific stress responses.
603
604 **Figure S3. Overlaps among the genes in cluster I-V. A-E.** Overlapping pie charts show the
605 levels of overlaps among genes in clusters I-V upon DHA, HS, and low-glucose treatments,
606 respectively.

607 **Table S1**. The transcriptomic changes in +aTc TetR-PfGCN5:GFP parasites at the ring stage under
608 stress conditions.

609 **Table S2**. The transcriptomic changes in TetR-PfGCN5:GFP parasites at the ring stage after KD
610 of PfGCN5.

611 **Table S3**. The transcriptomic changes in -aTc TetR-PfGCN5:GFP parasites at the ring stage under
612 stress conditions.

613 **Table S4**. Expression patterns by comparing -aTc and +aTc TetR-PfGCN5:GFP parasites under
614 three stress conditions.

Figure 1

A.

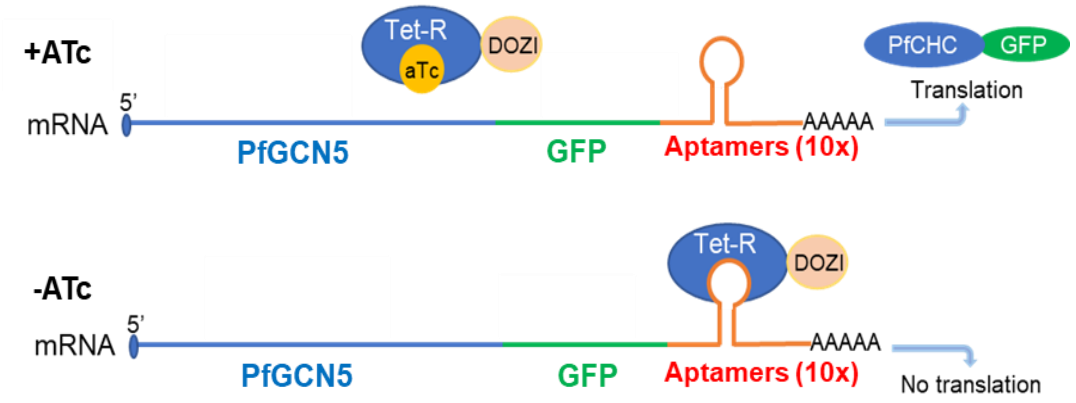

B.

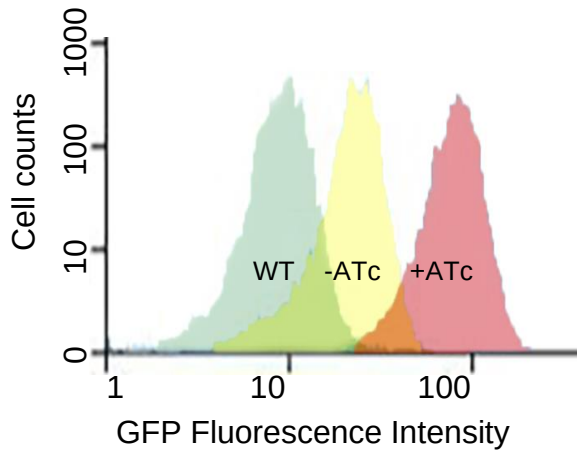

C.

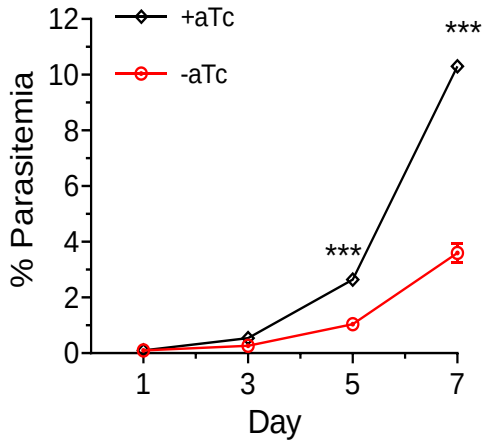

D.

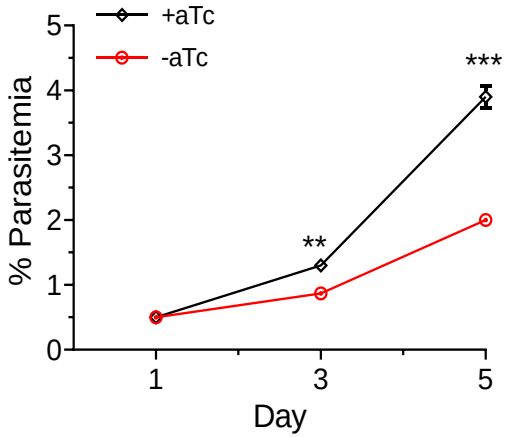

E.

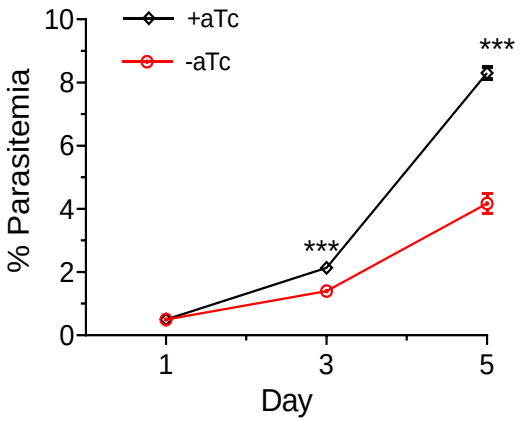

F.

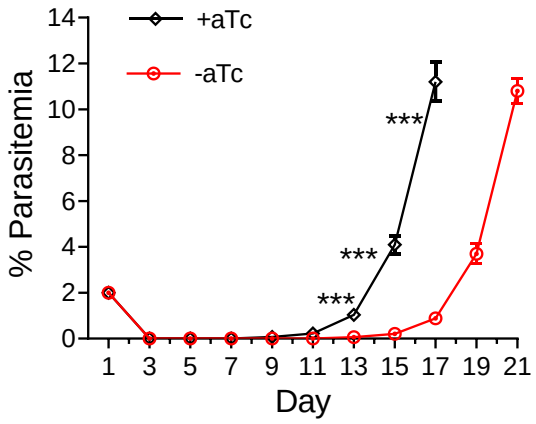

Figure 2

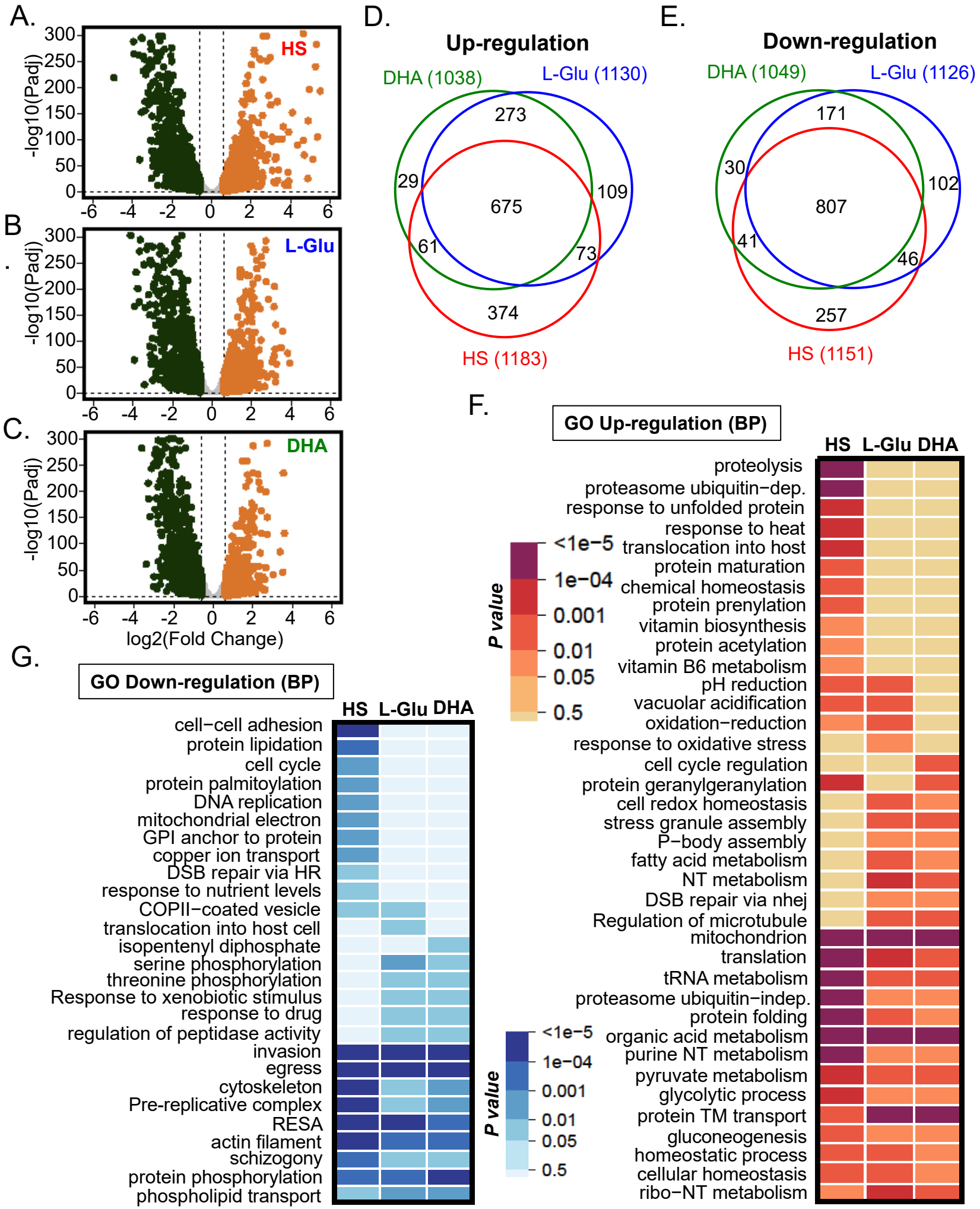
A.
HS
B.
L-Glu
C.
DHA
-log10(Padj)
log2(Fold Change)
D.
Up-regulation
DHA (1038)
L-Glu (1130)
HS (1183)
273
29
109
675
61
73
374
E.
Down-regulation
DHA (1049)
L-Glu (1126)
HS (1151)
171
30
102
807
41
46
257
F.
GO Up-regulation (BP)
HS L-Glu DHA
proteolysis
proteasome ubiquitin−dep.
response to unfolded protein
response to heat
translocation into host
protein maturation
chemical homeostasis
protein prenylation
vitamin biosynthesis
protein acetylation
vitamin B6 metabolism
pH reduction
vacuolar acidification
oxidation−reduction
response to oxidative stress
cell cycle regulation
protein geranylgeranylation
cell redox homeostasis
stress granule assembly
P−body assembly
fatty acid metabolism
NT metabolism
DSB repair via nhej
Regulation of microtubule
mitochondrion
translation
tRNA metabolism
proteasome ubiquitin−indep.
protein folding
organic acid metabolism
purine NT metabolism
pyruvate metabolism
glycolytic process
protein TM transport
gluconeogenesis
homeostatic process
cellular homeostasis
ribo−NT metabolism
P value
<1e−5
1e−04
0.001
0.01
0.05
0.5
G.
GO Down-regulation (BP)
HS L-Glu DHA
cell−cell adhesion
protein lipidation
cell cycle
protein palmitoylation
DNA replication
mitochondrial electron
GPI anchor to protein
copper ion transport
DSB repair via HR
response to nutrient levels
COPII−coated vesicle
translocation into host cell
isopentenyl diphosphate
serine phosphorylation
threonine phosphorylation
Response to xenobiotic stimulus
response to drug
regulation of peptidase activity
invasion
egress
cytoskeleton
Pre-replicative complex
RESA
actin filament
schizogony
protein phosphorylation
phospholipid transport
P value
<1e−5
1e−04
0.001
0.01
0.05
0.5

Figure 3

A.

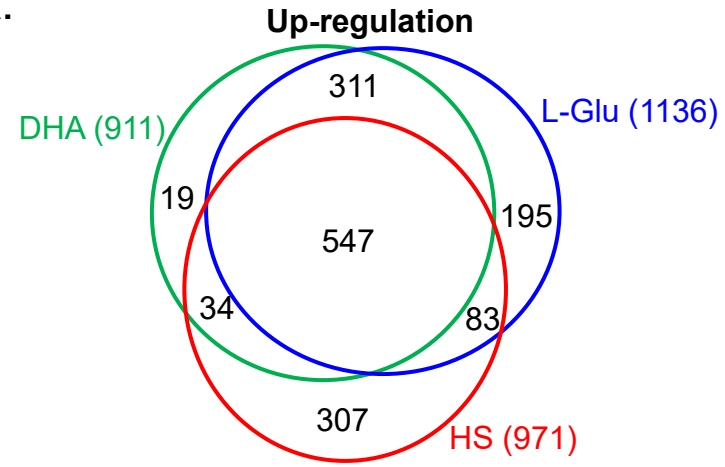

B.

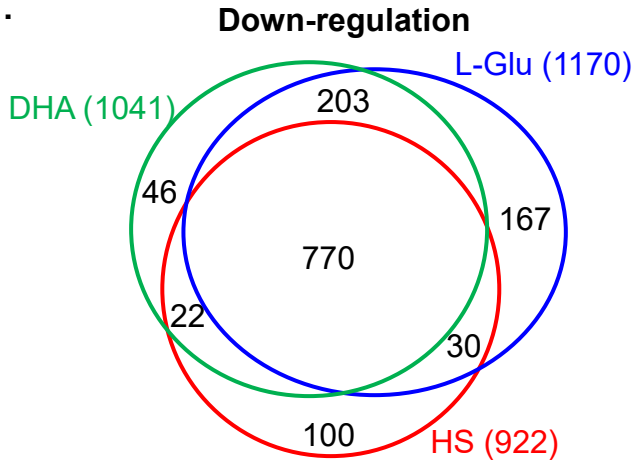

C.

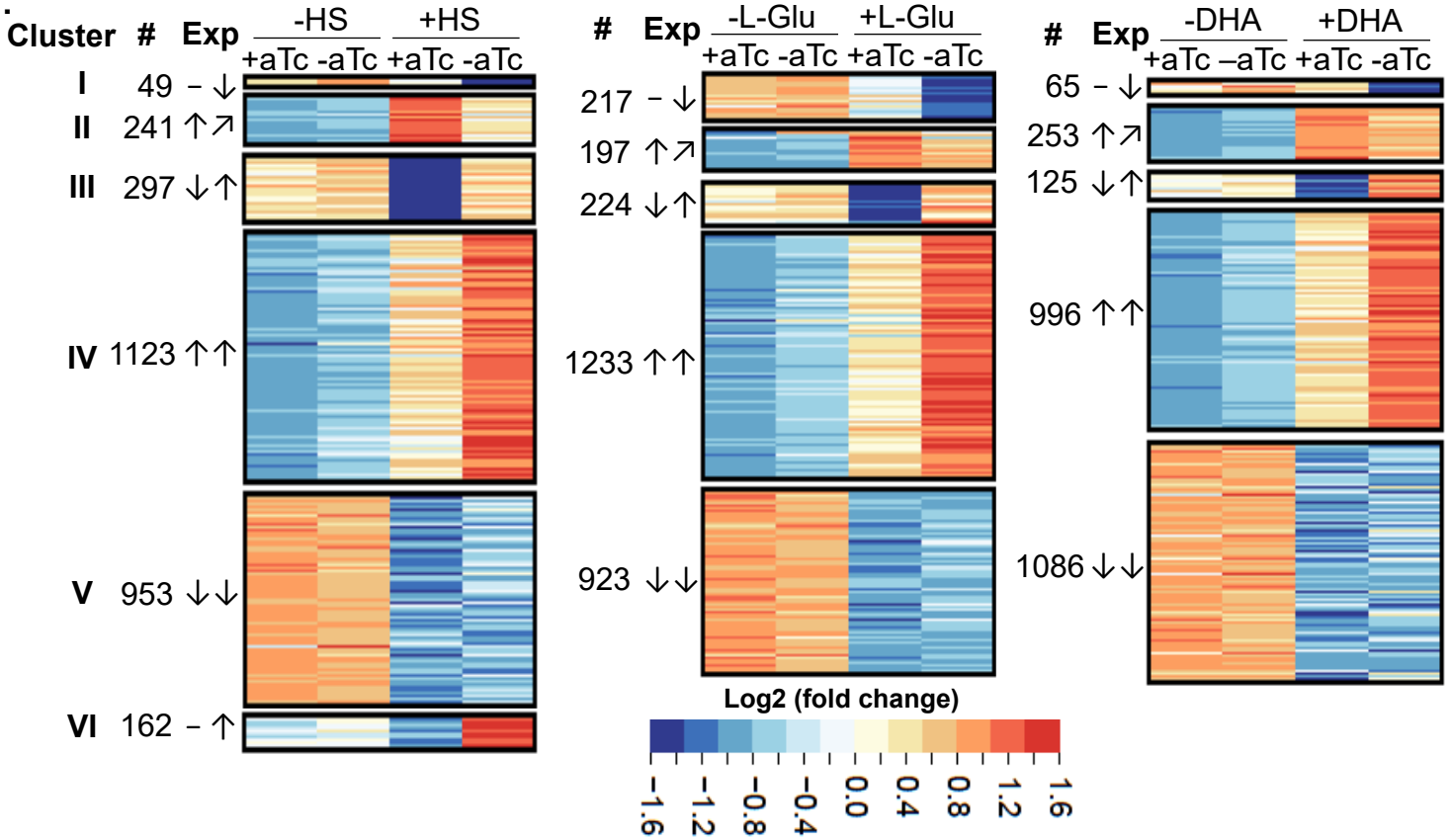

D.

Cluster	Heat shock, Low glucose, DHA treatment
I	**Ribosome biogenesis, GCN5, H3K4me3, response to drug, glutamine metabolism (KIC4)** HSP70 chaperone cycle, P-bodies, PTEX translocon, translation initiation
II	**Translation and ribosome, protein folding, tRNA process, ATP metabolic process, glycolysis, gluconeogenesis, ART proteome, response to drug xenobiotic stimulus, GARP, food vacuole, Sec61, PTEX translocon** Protein geranylgeranylation, proteasome assembly, mitochondrion transport and targeting, isoprenoid biosynthesis Cation homeostasis and pH reduction Hemoglobin digestion
III	**DNA replication and repair, cell cycle, isoprenoid biosynthesis, SERA** Cell adhesion, cytoskeleton organization, Mitochondrion electron transport
IV	**Proteasome, protein folding, mitochondrion, apicoplast, stress granule assembly, cytoskeleton organization, transport, fatty acid synthesis, gametocyte proteomics, ERAD** Response to heat and oxidative stress, ERAD, tRNA, amino acid and vitamin B6 metabolism, protein geranylgeranylation, microtube-based movement, cation homeostasis and pH reduction Response to ER stress and abiotic stimulus, cell redox homeostasis, cell cycle
V	**Entry into and exit from host, actin filament-based movement, endocytosis, protein modifications, food vacuole** Response to drug, lipid metabolic process Response to starvation, mRNA process, vesicle organization Response to drug and xenobiotic stimulus

Figure 4

A.

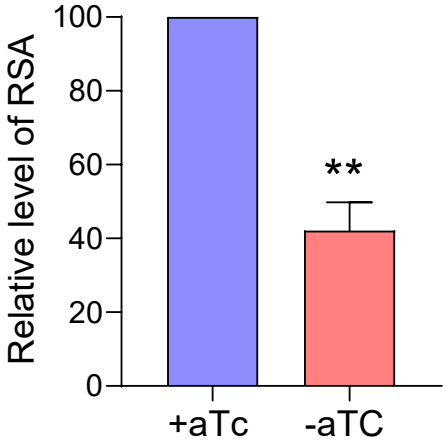
Relative level of RSA
100
80
60
40
20
0
**
+aTc
-aTC

B.

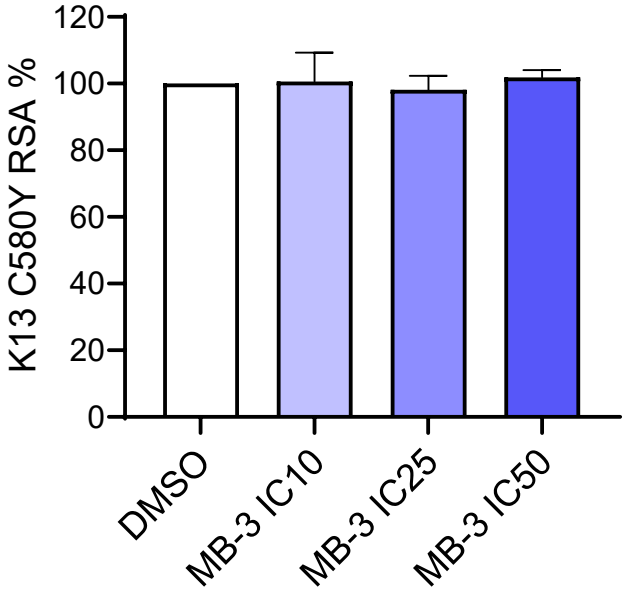
K13 C580Y RSA %
120
100
80
60
40
20
0
DMSO
MB-3 IC10
MB-3 IC25
MB-3 IC50

C.

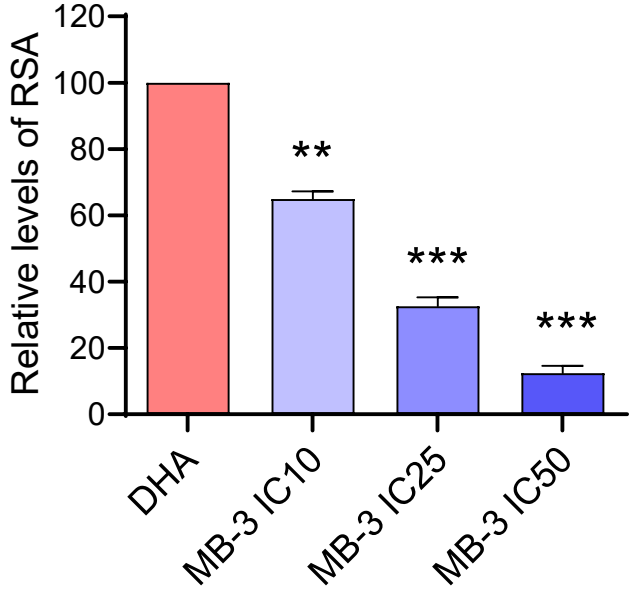
Relative levels of RSA
120
100
80
60
40
20
0
**
***
***
DHA
MB-3 IC10
MB-3 IC25
MB-3 IC50